An Extended and Improved Special Sensor Microwave Imager (SSM/I) Period of Record

HILAWE SEMUNEGUS

NOAA/National Climatic Data Center, Asheville, North Carolina

WESLEY BERG

Department of Atmospheric Science, Colorado State University, Fort Collins, Colorado

JOHN J. BATES AND KENNETH R. KNAPP

NOAA/National Climatic Data Center, Asheville, North Carolina

CHRISTIAN KUMMEROW

Department of Atmospheric Science, Colorado State University, Fort Collins, Colorado

(Manuscript received 8 June 2009, in final form 24 October 2009)

ABSTRACT

The National Oceanic and Atmospheric Administration National Climatic Data Center has served as the archive of the Defense Meteorological Satellite Program Special Sensor Microwave Imager (SSM/I) data from the *F-8*, *F-10*, *F-11*, *F-13*, *F-14*, and *F-15* platforms covering the period from July 1987 to the present. Passive microwave satellite measurements from SSM/I have been used to generate climate products in support of national and international programs. The SSM/I temperature data record (TDR) and sensor data record (SDR) datasets have been reprocessed and stored as network Common Data Form (netCDF) 3-hourly files. In addition to reformatting the data, a normalized anomaly (z score) for each footprint temperature value was calculated by subtracting each radiance value with the corresponding monthly 1° grid climatological mean and dividing it by the associated climatological standard deviation. Threshold checks were also used to detect radiance, temporal, and geolocation values that were outside the expected ranges. The application of z scores and threshold parameters in the form of embedded quality flags has improved the fidelity of the SSM/I TDR/SDR period of record for climatological applications. This effort has helped to preserve and increase the data maturity level of the longest satellite passive microwave period of record while completing a key first step before developing a homogenized and intercalibrated SSM/I climate data record in the near future.

1. Introduction

Measurements from the Defense Meteorological Satellite Program (DMSP) Special Sensor Microwave Imager (SSM/I) began in July 1987 and continue today, which make it the longest record of passive microwave satellite data. The SSM/I instrument is a seven-channel linearly polarized passive microwave radiometer that operates at frequencies of 19.36 (vertically and horizontally polarized), 22.235 (vertically polarized), 37.0 (vertically and horizontally polarized), and 85.5 GHz (vertically and horizontally polarized). Detailed specifications for the spacecraft and instrument are given by Colton and Poe (1999) and Raytheon (2000). The SSM/I was replaced by the Special Sensor Microwave Imager/Sounder (SSM/IS) in November 2005, although SSM/I is still operating. Eventually, the record of passive microwave instruments is planned to continue under the National Polar-Orbiting Operational Environmental Satellite System (NPOESS). SSM/I data are publicly available at National Oceanic and Atmospheric Administration (NOAA) National Climatic Data Center (NCDC) through the Comprehensive Large-Array Stewardship

Corresponding author address: Hilawe Semunegus, 151 Patton Ave., NOAA/National Climatic Data Center, Asheville, NC 28801-5001.
E-mail: hilawe.semunegus@noaa.gov

DOI: 10.1175/2009JAMC2314.1

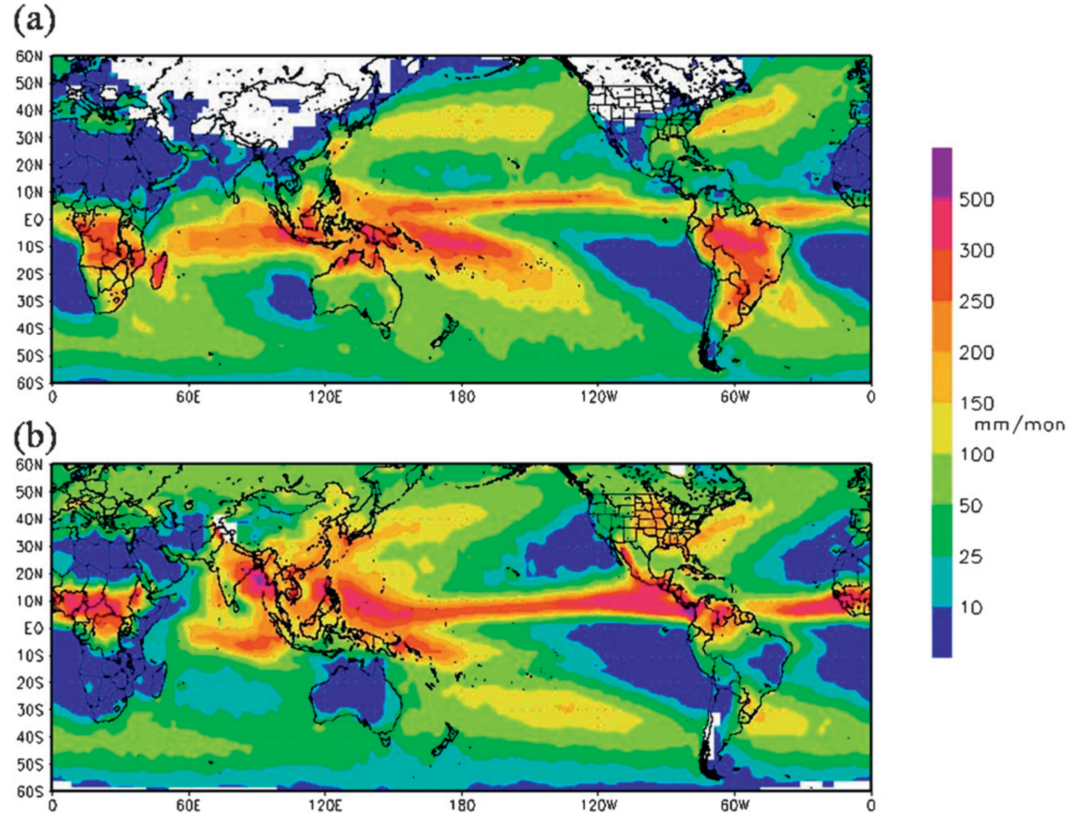

FIG. 1. Seasonal mean rainfall (mm month^{-1}) derived from 19 yr of SSM/I data for (a) December–February 1987–2006 and (b) June–August 1987–2006. (Courtesy of R. Ferraro, NOAA/STAR-CICS.)

System (CLASS). This paper addresses the techniques that have been applied to improve, extend, and reprocess the available SSM/I data from NCDC's archive.

SSM/I data measurements have been used extensively to generate climate datasets in support of both national and international programs. Ferraro et al. (1996) developed a set of hydrological products at 1° and 2.5° grid scales at the monthly time scale, which is used by a number of user groups to evaluate annual and interannual climate variability. NOAA utilizes these products, which are archived at the NCDC, to support its climate mission. An example of these products is shown in Fig. 1. In addition, the precipitation products generated as part of this project are one of the components of the Global Precipitation Climatology Project (GPCP; Huffman et al. 1996), which generates a suite of global precipitation products at daily to monthly time scales.

SSM/I data are also used by the cryospheric scientific community to monitor Arctic sea ice cover and detect contemporary changes in sea ice and ice sheets, which are critical for understanding the role of the Arctic in the global climate system (Serreze et al. 1990; Belchansky et al. 2005). Other applications that have been developed from SSM/I include the estimation of land surface temperature, soil moisture content, and oceanic surface wind speed (Weng and Grody, 1998; Jackson et al. 2002; Zhang et al. 2006).

To improve geophysical parameters such as global rainfall estimation in support of the National Aeronautics and Space Administration (NASA) Global Precipitation Mission (GPM), Berg and Kummerow (2006) developed SSM/I quality control procedures that have been shown to significantly remove spurious geolocation, radiance, and climatologically anomalous data. Vila et al. (2010) have demonstrated the effectiveness of these statistically based techniques, explained in this paper, to improve the quality of climatological precipitation products developed by Ferraro et al. (1996). Screening techniques have also been previously developed by Ferraro et al. (1998) to improve precipitation retrievals that use passive microwave data. Figure 2 shows the bias between the reprocessed (quality controlled) monthly rainfall estimates (expressed as millimeters per month) and the original for August 2005 using SSM/I antenna temperature data. Biases in long-trend analysis (1992–2007) were shown to be reduced by removing spurious values from the original antenna temperature data using data quality assessment methods described herein.

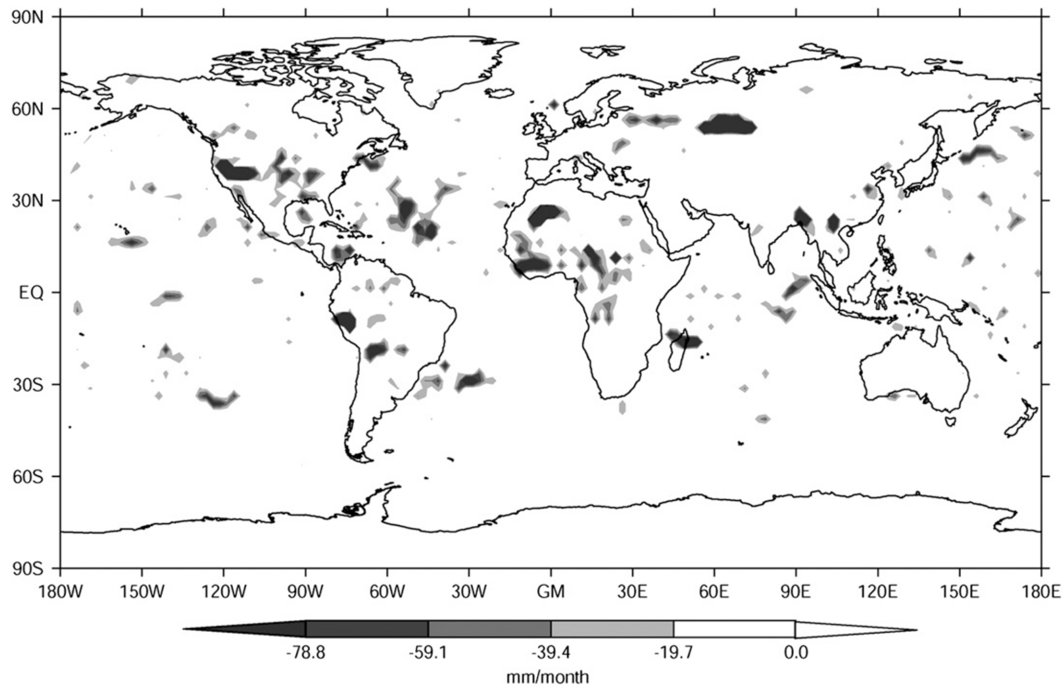

FIG. 2. Rainfall bias between reprocessed values and the original dataset for August 2005. Negative values indicate that original values are larger than reprocessed values. (Vila et al. 2010).

The primary objective of this paper is to describe a SSM/I dataset that is sufficiently quality controlled to enable climate data record (CDR) development through NOAA's Scientific Data Stewardship (SDS) program (National Research Council 2004) and to improve current SSM/I antenna and brightness temperature products. As shown in Fig. 3, a fundamental climate data record (FCDR) composed of an intercalibrated and homogenized SSM/I time series (July 1987–present) will be developed and made publicly available. FCDR development will address issues such as intersensor and cross-sensor calibration, cross-track bias corrections, radar-calibration (RADCAL) beacon interference, orbital drift, and navigational inaccuracies; however, such development is beyond the scope of this paper. This paper aims to identify and analyze SSM/I radiance data quality issues and detail the statistical quality control techniques that were developed to address these problems. This is a key first step in developing a SSM/I FCDR that identifies and mitigates serious radiance errors in the temperature data record (TDR; or antenna temperatures) and sensor data record (SDR; or brightness temperatures).

2. Methodology

All native or original SSM/I TDR and SDR data used as input for this study were originally received and processed by the U.S. Navy's Fleet Numerical Meteorology and Oceanography Center (FNMOC) and the U.S. Air Force Weather Agency (AFWA). All data referenced in this paper are from the seven channels that were measured from SSM/I instruments flown on *F-8*, *F-10*, *F-11*, *F-13*, *F-14*, and *F-15* satellites: the 19-GHz vertical and horizontally polarized (19V and 19H, respectively), the 22-GHz vertically polarized (22V), the 37-GHz vertically and horizontally polarized (37V and 37H), and the 85-GHz vertically and horizontally polarized (85V and 85H) data. To improve the SSM/I dataset at the file level, steps were taken that addressed previously unreadable or unrecognizable SSM/I data, duplication of scans, and inconsistent temporal sampling intervals. Collaborative efforts between NCDC and the Colorado State University (CSU) have led to the rescue and extension of the SSM/I period of record by approximately 7 yr (July 1987–August 1993) to complete the period of record. SSM/I data were reprocessed to identify suspicious or erroneous data through the use of temperature, climatology, geolocation, and temporal flags that were then embedded in a self-describing standard format.

a. File-level improvements

For SSM/I data prior to 1998, 2140 orbital files (1.4% of the total number of SSM/I files in CLASS) were flagged as having a mismatch between the file-naming information and the data header record inside the file. Of these, about half (50.9%) were caused by mismatches in

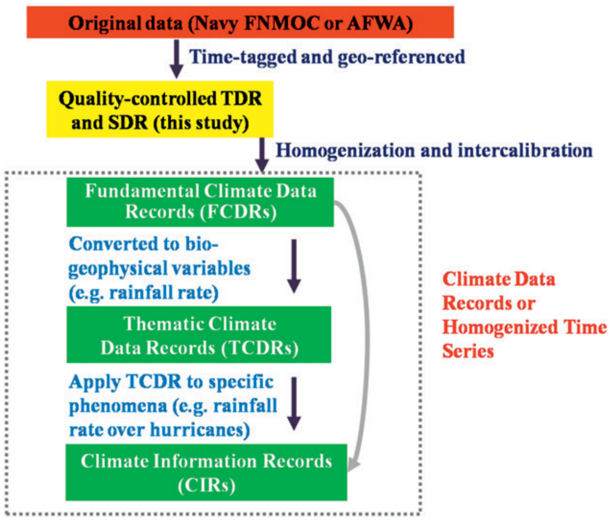

FIG. 3. Flowchart for the development of a SSM/I CDR. FCDRs refer to a homogenized and intercalibrated radiance time series. TCDRs are the biogeopyhsical variables or products that are derived from FCDRs.

satellite type (e.g., *F-8*) and data record type (either TDR or SDR). After data header record information was verified, the files were renamed to include the appropriate satellite name and data record type and placed into the NCDC archive. The remaining 1051 flagged files (0.7% of the total number of SSM/I files in the CLASS archive) were excluded from the SSM/I period of record for having either an unreadable or unrecognizable data header–record structure.

SSM/I data also have overlapping or duplicative scans (FNMOC processing design), particularly at the start and end of each file. These overlapping times range from a few minutes to several hours of data. Over the entire SSM/I period of record, these overlapping times constitute 5% of the data. To avoid duplication of data points for scientific research, this problem was addressed by taking all of the SSM/I TDR or SDR data for a whole day for a given satellite and record type and keeping the first instance of a duplicative data occurrence. In this way, each scan represents a unique temperature record for a corresponding time and geolocation, which is important for accurately estimating geophysical parameters on a climatological scale. In this study, eight files per satellite per day were produced for SSM/I data because 3-hourly intervals (e.g., 0000–0259 UTC) facilitate temporal subsetting and record-keeping purposes. Previously, original orbital files started and ended at unpredictable or nonpredetermined times.

b. Reprocessed data

While reading SSM/I data prior to 1998, corrupted data scans were observed in the SSM/I data. Many of these corrupted scans caused read routines to fail and incomplete data to be read and collected. Data were reformatted (or reprocessed) to ensure that only "good" data were read and inventoried by CLASS in order to preserve uncorrupted original data, to include quality flags as variables (as explained in later sections), and to rewrite data in a self-describing, widely used and user-friendly format. It was decided that the network Common Data Format (netCDF), which conforms to Climate and Forecast (CF), version 1.4, conventions or standards, would be utilized (Lawrence Livermore National

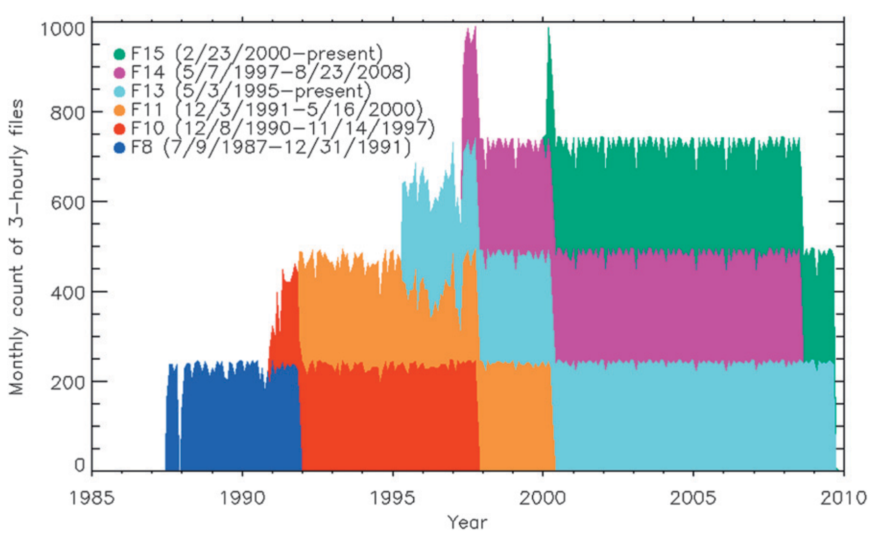

FIG. 4. Monthly count of 3-hourly netCDF SSM/I TDR or SDR data obtained from the various satellites. The *F-13* and *F-15* SSM/I instruments are the last active platforms, as of 7 Oct 2009.

Laboratory 2009). NetCDF is a set of software libraries and machine-independent data formats that support the creation, access, and sharing of array-oriented scientific data with various publicly available tools for manipulating and displaying data (UCAR Unidata 2009). SSM/IS TDR and SDR data have also been converted to netCDF-CF in a 3-hourly format (available through CLASS) without overlapping times, but did not have any quality control procedures applied to them and are not described further in this paper.

c. *Extending period of record available*

As a result of the file quality assessment above, the netCDF SSM/I period of record of publicly available data from NOAA's CLASS (online at http://www.class.noaa.gov), the storage support system for NCDC, was extended back to 9 July 1987 (as shown in Fig. 4), whereas the previous start data for SSM/I data in CLASS was 17 February 1997. SSM/I data prior to August 1993 were recovered from multiple sources, including NOAA's Center for Satellite Applications and Research (STAR) and Earth System Research Laboratory and CSU, and were added to the netCDF SSM/I period of record.

d. *Antenna pattern corrections*

Antenna temperature or TDR data are converted to brightness temperature or SDR data by applying an antenna pattern correction (APC). Once raw antenna temperatures are calculated by FNMOC they must be corrected for the antenna pattern to produce the brightness temperatures given in the SDRs. As energy from a particular scene station (or footprint) is sampled by the sensor, additional energy is measured resulting from the antenna sidelobe pattern. To remove the effect of the sidelobes, an APC is performed on each sample. To correct a particular channel at a given scene station, the adjacent along-scan scene stations and the cross-polarization term at the current scene station are used to remove the energy contributed by the sidelobes (Raytheon 2000). The APC coefficients used to calculate the brightness temperatures are provided in Table 1. These coefficients are the corrected and more up to date compared to the APC coefficients found in Colton and Poe (1999). The APC calculations [Colton and Poe 1999, their Eq. (3)] and Table 1 coefficients were used to generate SDRs for both the native and 3-hourly netCDF SSM/I SDR period of record. The same coefficient values for *F-13*, *F-14*, and *F-15* satellites are used for Table 1, which are different than the ones found in Colton and Poe (1999; G. Poe 2003, personal communication). Brightness temperature values from the FNMOC/AFWA SSM/I SDR dataset and netCDF SSM/I SDR dataset were compared and found to be identical.

TABLE 1. Updated antenna pattern correction coefficients for each SSM/I platform and channel (G. Poe 2003, personal communication). Channels 1–7 (second column) correspond to the following frequency–polarization order: 19V, 19H, 22V, 37V, 37H, 85V, 85H.

Satellite	Channel	Coef 1	Coef 2	Coef 3	Coef 4
F-8	1	1.047 10	−0.004 90	0.007 30	−0.002 90
	2	1.047 20	−0.004 30	−0.008 00	−0.002 80
	3	1.051 30	−0.011 10	−0.008 00	−0.005 50
	4	1.042 20	−0.022 50	−0.003 20	−0.002 20
	5	1.042 80	−0.027 20	−0.001 00	−0.000 40
	6	1.034 10	−0.014 20	−0.004 00	−0.003 70
	7	1.015 80	0.000 00	−0.002 70	−0.000 90
F-10	1	1.045 70	−0.004 30	−0.005 50	−0.003 90
	2	1.050 40	−0.008 60	−0.007 30	−0.002 60
	3	1.045 10	−0.007 20	−0.006 00	−0.005 20
	4	1.040 70	−0.024 40	−0.001 00	−0.001 00
	5	1.036 00	−0.020 50	−0.000 30	−0.001 00
	6	1.048 20	−0.023 60	−0.008 30	−0.004 10
	7	1.049 40	−0.028 80	−0.006 70	−0.001 80
F-11	1	1.041 00	−0.004 10	−0.002 83	−0.002 08
	2	1.044 13	−0.003 81	−0.003 74	−0.003 52
	3	1.045 11	−0.007 35	−0.003 23	−0.002 55
	4	1.036 22	−0.020 67	−0.001 31	−0.001 11
	5	1.039 48	−0.020 16	−0.001 94	−0.002 11
	6	1.040 42	−0.027 34	−0.001 04	−0.000 98
	7	1.038 78	−0.022 53	−0.001 52	−0.001 52
F-13, *F-14*, and *F-15*	1	1.043 28	−0.005 73	−0.003 21	−0.002 34
	2	1.042 38	−0.004 43	−0.003 58	−0.003 45
	3	1.044 89	−0.005 49	−0.002 45	−0.002 80
	4	1.039 10	−0.020 97	−0.000 91	−0.000 98
	5	1.039 23	−0.018 76	−0.001 51	−0.001 65
	6	1.042 92	−0.028 10	−0.001 82	−0.001 82
	7	1.024 74	−0.012 15	−0.001 82	−0.001 72

e. *Statistically based quality control procedures*

Major errors that were found relating to footprint-level geolocation, time, and radiance values in the SSM/I TDR/SDR period of record were identified through the use of quality flags embedded in each 3-hourly netCDF file. The flagged data include the following:

- latitudinal and longitudinal values were found to be out of range of $-90° <$ latitude $< 90°$ and $-180° <$ longitude $< 180°$,
- interscan line distances were not realistic (the distance between individual pixel values along a scan or footprints should be between 10 and 30 km),
- time values were found to be outside the range of actual start and end times, and
- antenna or brightness temperatures were outside the range from 50 to 325 K.

Applying threshold quality flags was the simplest solution to identify some errors found in SSM/I data, but was not adequate to identify all of the potential spurious data.

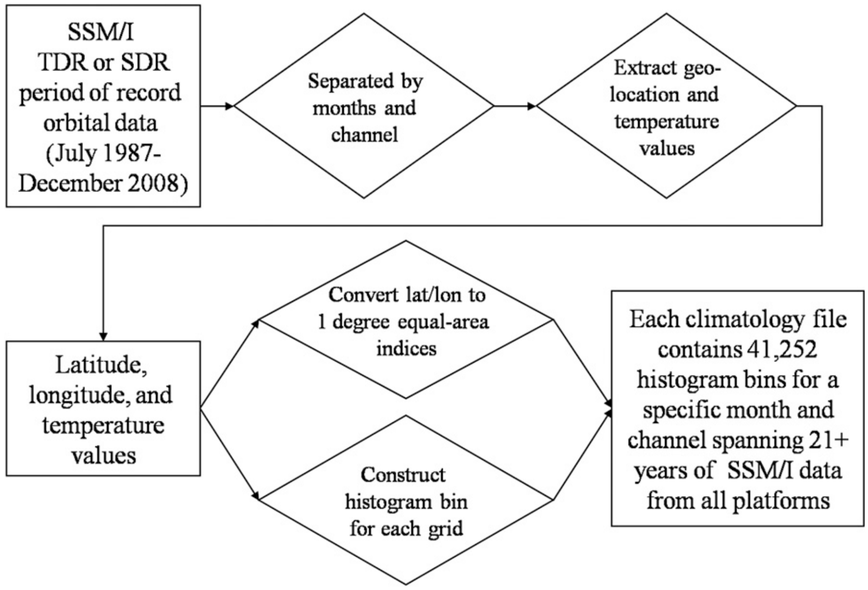

FIG. 5. Flowchart depicting the methods used to create a climatology file.

To address suspicious or erroneous data that could not be corrected through these threshold-based quality flags, a climatology quality flag was developed. This quality flag determined whether SSM/I footprints were consistent with the climatological record of the entire SSM/I period of record at a given location. Figure 5 summarizes the algorithm for the creation of climatology files. For both the SSM/I TDR and SDR datasets, climatology files were developed for each month and channel (e.g., 19V) using the satellite period of record. Geolocation values were converted to 1° equal-area grid indices (41 252 grid boxes). For each file associated with a specific month and channel, the channel data were tallied to construct a histogram for each grid box. The resultant files encompassed channel data (either TDR or SDR) across all platforms and grid boxes for each month and each channel. Climatology files were processed at the end of every year to extend the current climatological period of record (July 1987–December 2008) with newly archived data.

Figure 6 depicts how climatology files are used to detect anomalies in footprint-level data from the original SSM/I TDR/SDR data. For each SSM/I TDR or SDR orbital file, the corresponding climatology file is found based on filename information about the data type and month of the orbital file. Geolocation values from the orbital file are converted to grid indices in order to match the orbital geolocation values with the appropriate climatology gridbox histogram. The corresponding channel data are also extracted for the orbital file. The climatology file's histogram for the appropriate grid box is then used to calculate channel mean and standard deviation statistics. Normalized anomalies were calculated by subtracting the climatological means and dividing by the climatological standard deviation (i.e., a statistical z score). Normalized anomalies with absolute values greater than 10 were flagged as either being suspicious or having possible errors. This z-score threshold was found to be a reliable indicator of suspicious or erroneous data (as shown in later sections), but in order to provide user options for choosing a custom z-score threshold, z-score values (corresponding to each antenna or brightness temperature value) at the footprint level are also included as variables in each 3-hourly SSM/I netCDF file. Figure 7 summarizes how SSM/I TDR and SDR datasets have been improved by the steps described above.

3. Results and discussion

a. Data gaps and availability

Data gaps and limited availability of archived SSM/I data for certain time windows were commonly observed in the period of record. The causes of these gaps or the limited number of SSM/I data have not been adequately explained through previous literature. A major data gap was observed from 1 December 1987 through 12 January 1988 for the *F-8* SSM/I record, which can be seen in Fig. 4 on a monthly count scale. A significant *F-10* SSM/I data gap occurred from 29 March 1991 to 18 April 1991, and a smaller gap was observed from 6 December 1991 to 11 December 1991. Three notable *F-11* SSM/I data

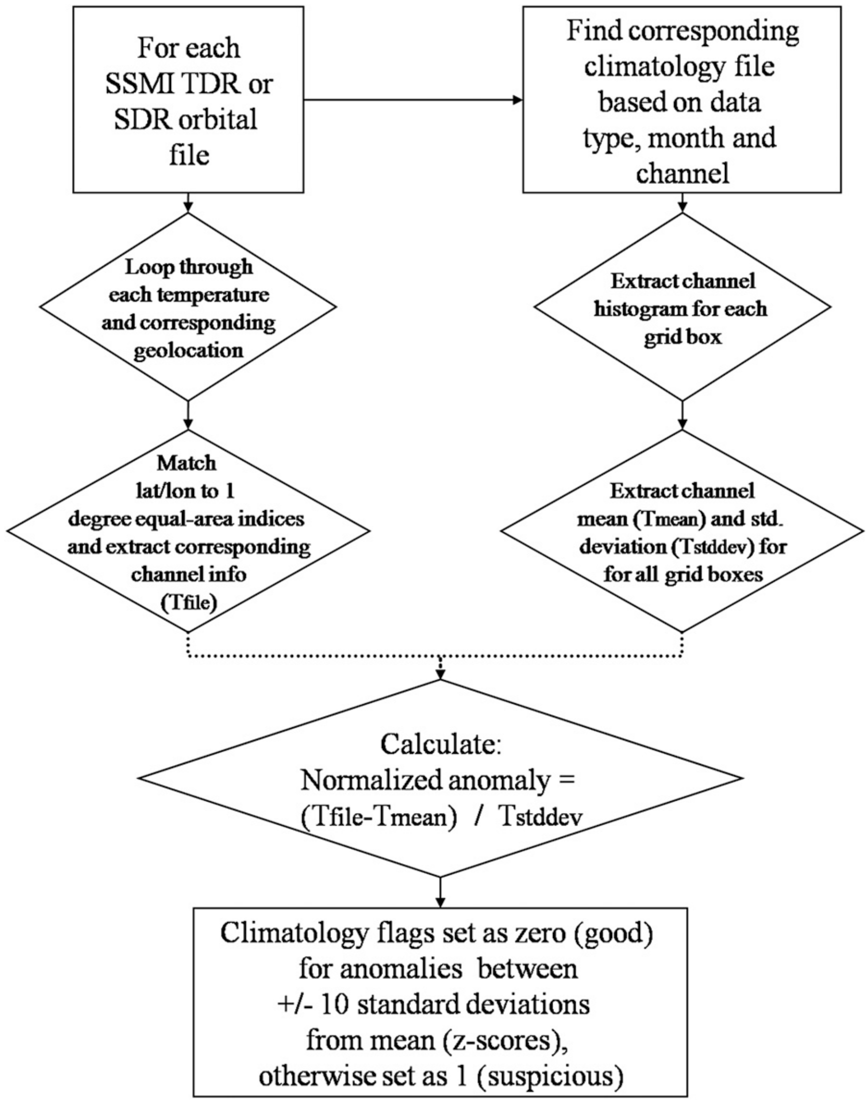

FIG. 6. Schematic of climatology quality flag application of original SSM/I data.

gaps were found from 31 May 1996 to 6 June 1996, from 19 February 1997 to 28 February 1997, and more significantly from 18 March 1997 to 21 April 1997. Figure 4 also shows that *F-11* SSM/I data were not fully archived between 1995 and 1998. Similar gaps with *F-10* and *F-13* data lead us to speculate that this prolonged data shortage may be due to the limited storage and/or processing capability of ingesting SSM/I data from three satellites by FNMOC or AFWA during that period.

b. SSM/I data analysis by satellite

Calculation of each SSM/I channel involves converting the sensor voltages (cold and warm calibration counts) into antenna temperatures incident on the antenna feed horn, which is explained in full detail by Raytheon (2000). SSM/I observations of antenna temperature data showed that the onboard cold and warm calibration counts were the best indicators of instrument health or radiance data quality from all satellites (Raytheon 2000). Erratic calibration count readings coincided with suspicious or erroneous antenna or brightness temperatures. Large numbers of scattered, disconnected, and suddenly rising or falling calibration counts are common in the SSM/I period of record. For the most part, the exact reasons for instrument failure and cold–warm calibration fluctuations have rarely been explained through publicly available literature (Raytheon 2000).

1) *F-8* SATELLITE

Both the 85H and 85V channels failed (85V in February 1989 and 85H in October 1990) aboard the *F-8* satellite,

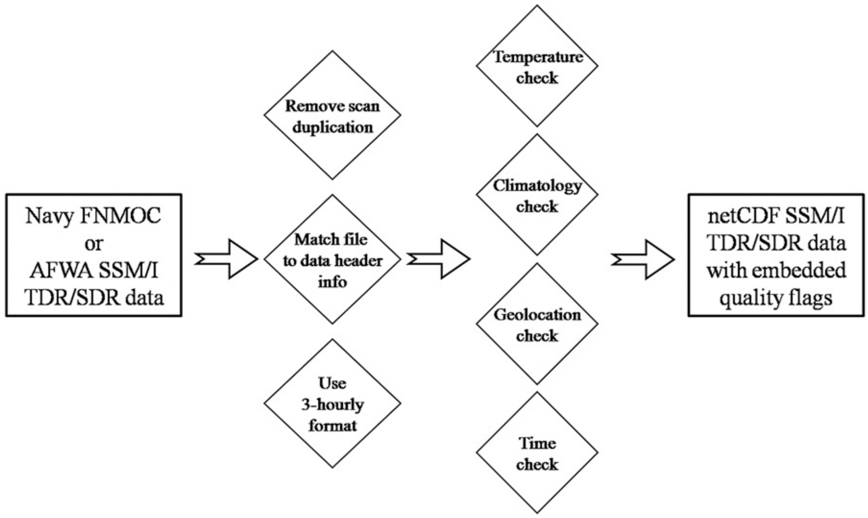

FIG. 7. Overall steps taken to create the netCDF SSM/I period of record.

most likely due to overheating of the radio frequency (RF) electronics (Raytheon 2000). According to Raytheon (2000), both channels had noise levels that gradually increased in an inconsistent manner until the signal from Earth was completely obscured. However, calibration counts from the 85H and 85V channels (Figs. 8a,b, respectively) show that erratic calibration count readings first occurred in January 1988. Figure 8c,d provides the

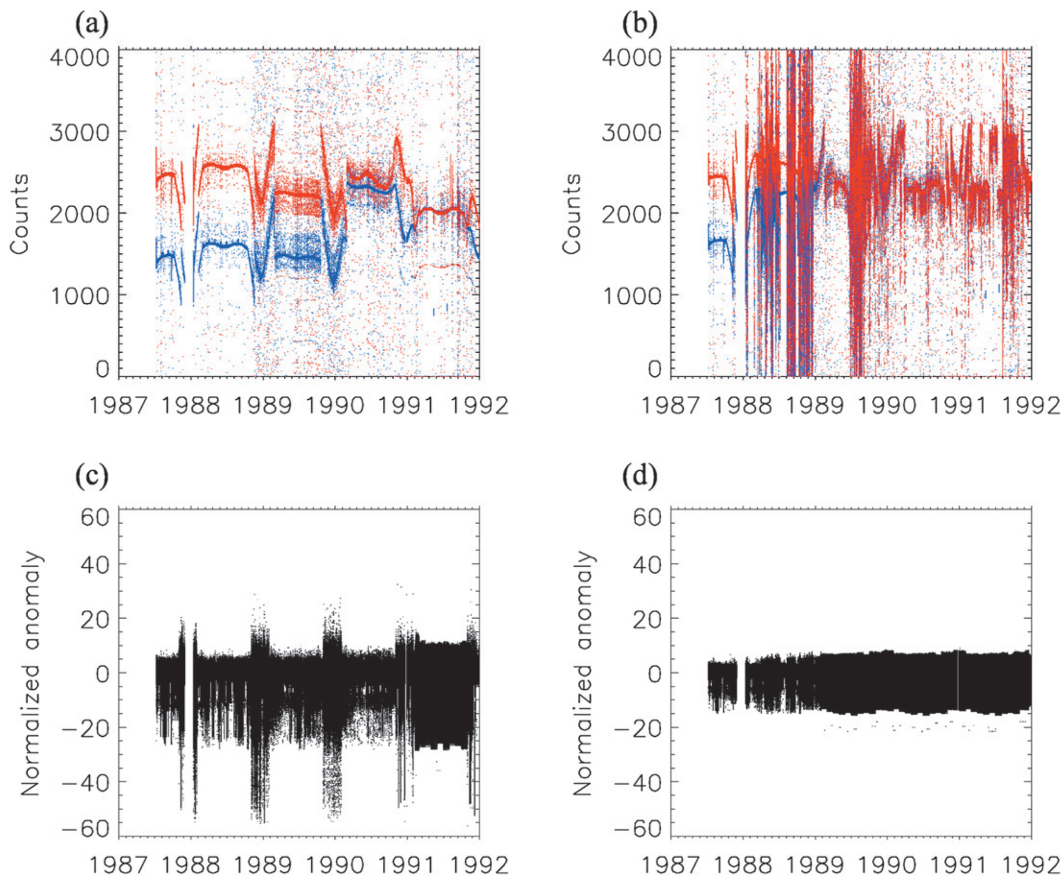

FIG. 8. Cold (blue dots) and warm (red dots) calibration counts for the (a) 85H and (b) 85V channels. (c),(d) Normalized anomalies or z scores for the same channels.

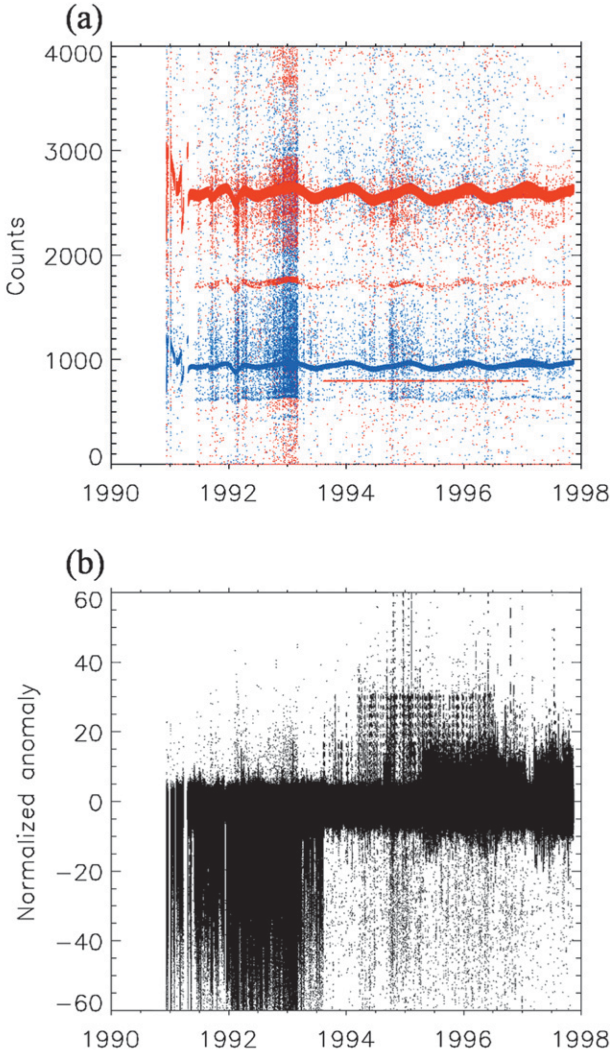

FIG. 9. (a) Calibration counts and (b) corresponding z scores for the *F-10* 19V channel.

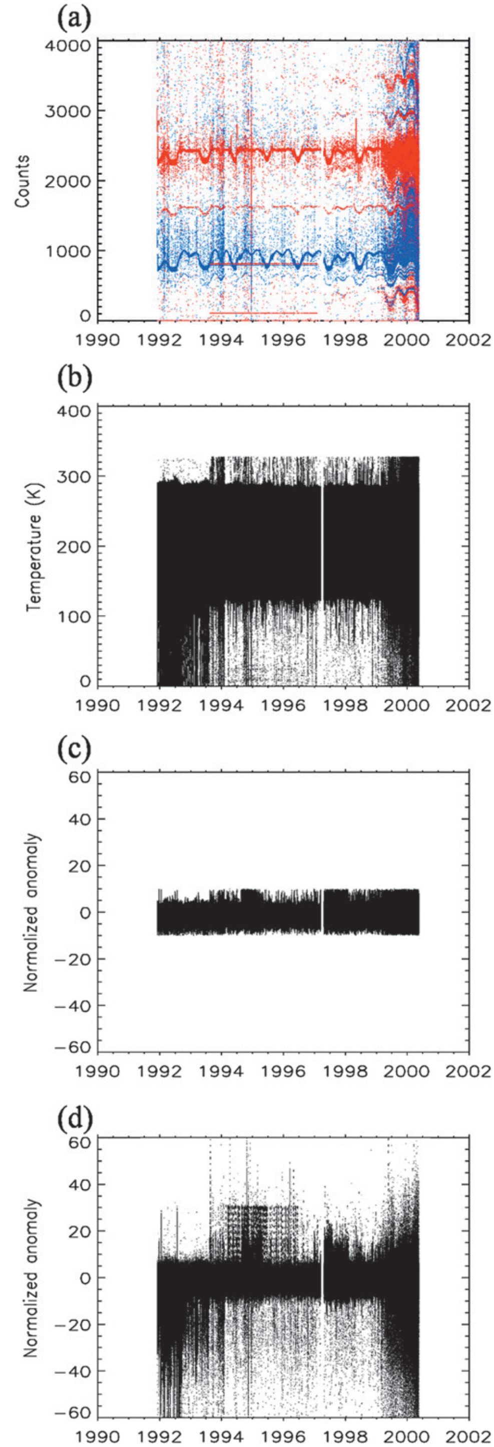

FIG. 10. (a) Calibration counts, (b) corresponding z scores, and (c) temperatures for the *F-11* 37H channel.

corresponding z scores that were calculated for those channels and shows that anomalous antenna temperature data ($-10 < z$ score < 10) were persistent throughout the entire 85H and 85V records. For the 85H channel, anomalous data were of a higher magnitude whenever the cold/warm calibrations strongly shifted or made sudden jumps; in February 1991, this channel was completely saturated (block-filled area) and severely degraded for the rest of the 85H record. For the 85V channel, the z scores were either within or slightly outside of the ± 10 threshold limit, but antenna temperatures became saturated and unusable earlier in December 1988 (compared to 85V z scores) through the rest of the 85V channel record. For both channels, the z-score method complemented and provided additional information about the health of the *F-8* SSM/I 85H and 85V channels. Because of 85H and 85V channel degradation, temperature data from the 85V and 85H channels for the *F-8* satellite are not included in precipitation products in Ferraro et al. (1996) and Vila et al. (2010).

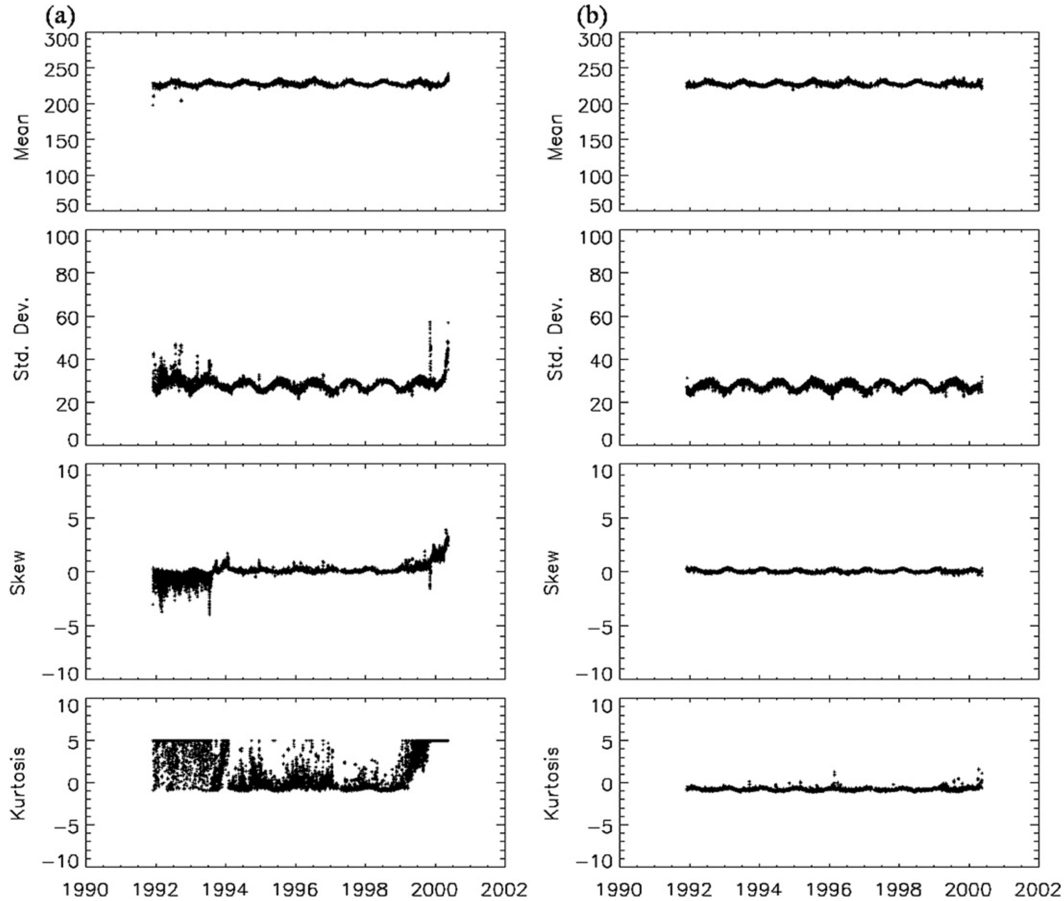

FIG. 11. Statistical moments for the *F-11* 22V channel (a) without quality flags applied and (b) with all quality flags applied: (top to bottom) mean, std dev, skewness, and kurtosis. Notice how the known instrument failure period after 1998 is improved for (b).

The z scores for the other *F-8* channels were routinely outside the ± 10 threshold but did not display any of the serious channel degradation found in the 85H and 85V channels.

2) *F-10* SATELLITE

Figures 9a,b illustrate *F-10* 19V calibration counts and corresponding z scores, respectively, which were representative of calibration count and z-score features found in the other six channels. All of the *F-10* SSM/I channels exhibit a similar jump in cold and warm calibration counts in March/April 1991 and a general wide scatter of data from the beginning of the period of record through August 1993 for both calibration counts and z scores. The z scores outside ± 10 appeared to identify most of these anomalous data. Figures 9a,b also show that there were additional or secondary solid warm or cold calibration lines for the 19V channel in 1994. There were also positive trends in cold–warm calibration counts only for the 19H, 22V, and 85V channels over the *F-10* period of record. All of the channels showed noisy positive anomalous signals (Fig. 9b), especially from 1994 through early 1997, with z-score trends then stabilizing until the *F-10* SSM/I instrument was decommissioned.

3) *F-11* SATELLITE

Figures 10a–d show cold/warm calibration counts, anomalies (before and after the z-score threshold of ± 10 is applied), and temperatures, respectively, for the *F-11* SSM/I 37H channel. All of the other channels display nearly identical features; thus the Fig. 10 plots are representative of all *F-11* SSM/I channels. Calibration count, z scores, and antenna temperatures showed noticeable scatter from 1992 through mid-1996 and considerable instrument health issues starting in 1999, culminating in total instrument failure in May 2000. Frequent temperatures excursions, defined as temperatures below 50 K or above 325 K, were observed during the 1999–2000 period. Corresponding z scores (Fig. 10b) show more nuanced temperature variations, which allowed for a better understanding of potentially suspicious or erroneous data, compared with using simpler temperature thresholds. In addition, when a z-score threshold of ± 10 was employed as shown in Fig. 10c, most of the errors in the *F-11* data were identified and removed. Figure 11 shows statistical moments (mean, standard deviation, skew, and kurtosis) for each 3-hourly netCDF SSM/I *F-11* SDR file, both without (Fig. 11a) and with (Fig. 11b) quality flags applied. Both climatology and threshold flags were applied for Fig. 11b. A noticeable improvement for both the early and latter problematic period of the *F-11* SSM/I instrument is shown through this analysis. However, some of the *F-11* temperature anomalies in late 1999 and 2000 can still be observed on a smaller scale.

4) *F-13* SATELLITE

Figures 12a–d illustrate cold/warm calibration counts, z scores, climatology, and temperature exceedances, respectively, for the *F-13* SSM/I 19H channel, which was representative of errors found in the rest of the channels. Climatology exceedances show the percentage of z-score values (footprint level) that were less than -10 and greater than 10 in each 3-hourly netCDF TDR file (Fig. 12c). Similarly, temperature exceedances were defined as the percentage of temperatures that were below 50 K and above 325 K. Cold and warm calibration counts shown in Figs. 12a,b show mostly reliable instrument health from May 1995 through 1998. Sharp but brief jumps were followed by major errors in calibration count readings in late 2003 through 2007. This late 2003–07 period can also be observed for the *F-14* and *F-15* SSM/I instruments [see sections 3(b)5 and 3(b)6], which indicates that this period may be attributed to FNMOC ground feed station processing issues that were not documented nor reported through publicly available literature. After 2007, calibration count readings mostly stabilized but large scatter was still found to be present. The climatology exceedances showed that the use of z scores within ± 10 was a good indicator of potentially erroneous data. Temperature exceedances captured most of the major error periods found in the calibration readings, but poorly characterized some of the smaller suspicious data during the periods of 1997–98 and 2002.

5) *F-14* SATELLITE

Calibration readings and z scores from the *F-14* 37H channel, which were representative of other *F-14* SSM/I channels, showed that between late 2003 and 2008, there were major issues with cold and warm calibration counts (Fig. 13a) and z scores (Fig. 13b) for the *F-14* 19H channel. There were also z-score anomalies at the beginning of the *F-14* SSM/I period of record in early 1997 through mid-1999. Similar to *F-13* SSM/I channels, the quality of radiance data after 2007 improved, but errors in the calibration readings were still found to exist until the

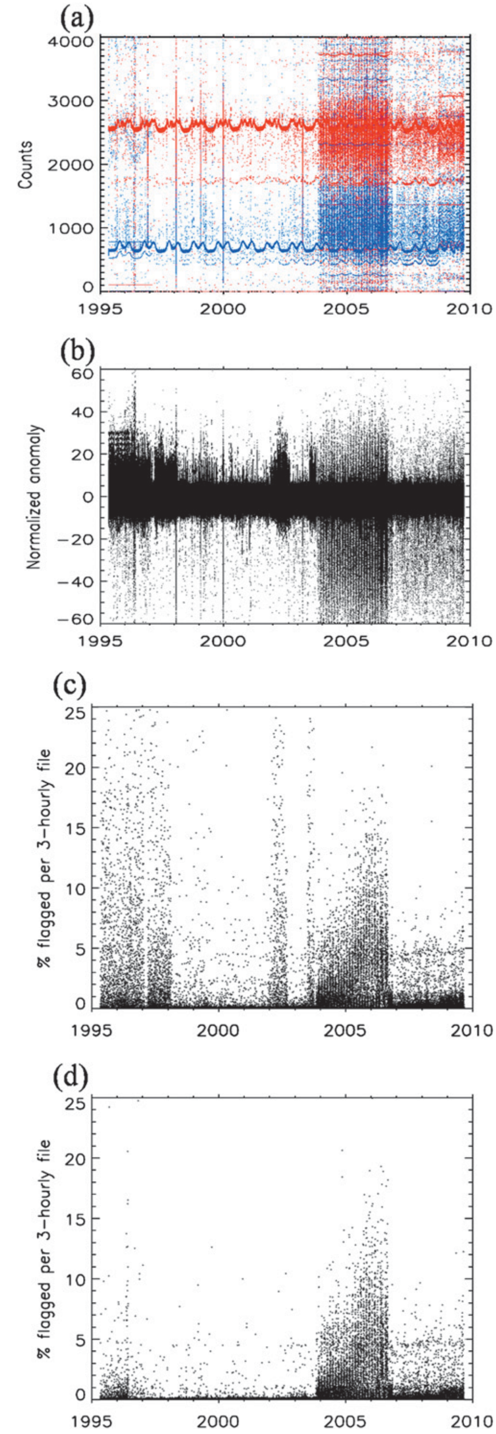

FIG. 12. (a) Calibration counts, (b) z scores, (c) climatology, and (d) temperature exceedances for the *F-13* 19H channel.

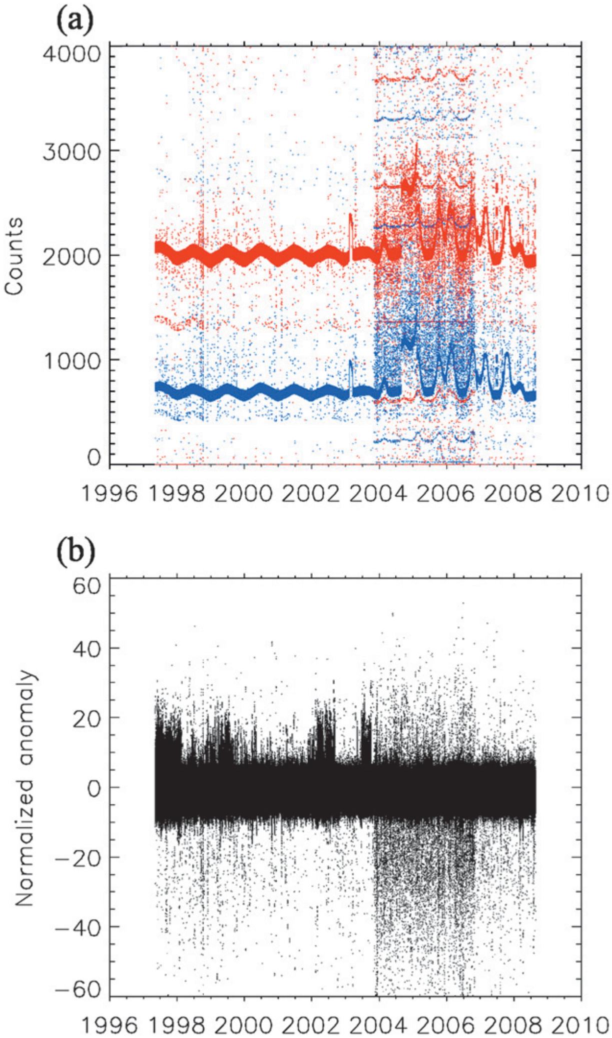

FIG. 13. (a) Calibration counts and (b) z scores for the *F-14* 37H channel.

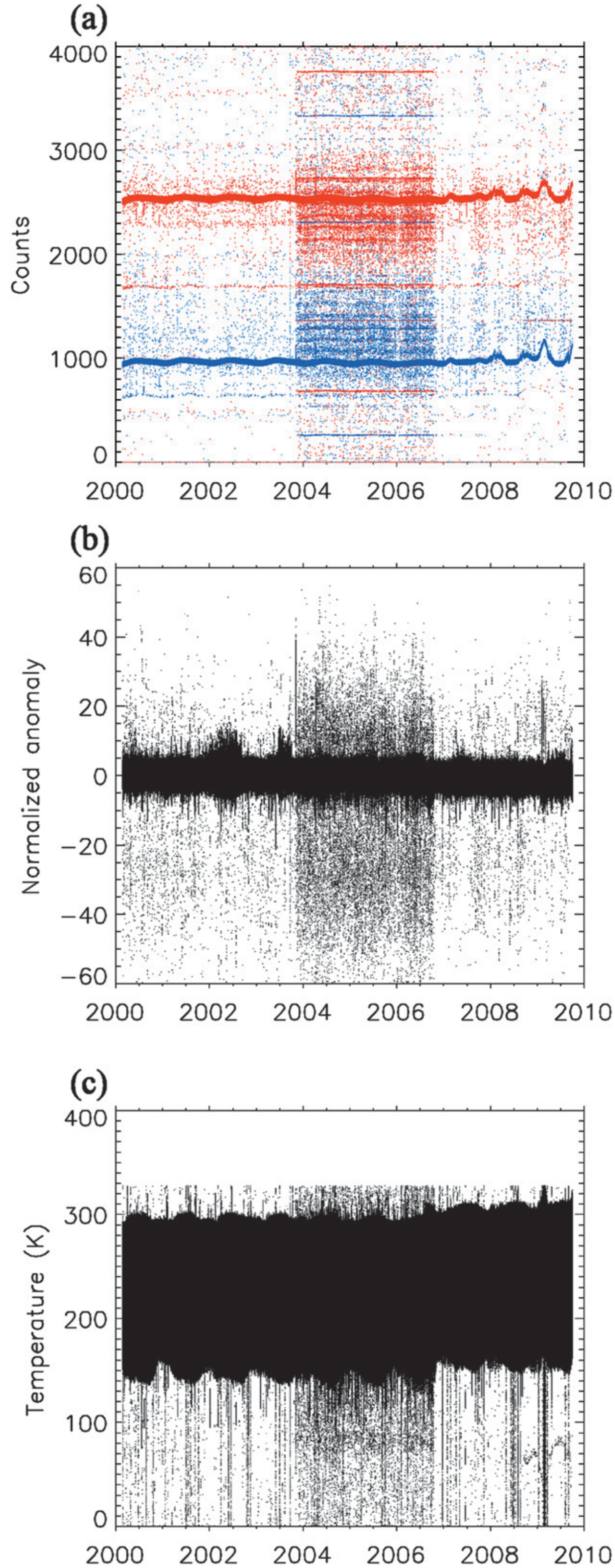

FIG. 14. (a) Calibration counts, (b) z scores, and (c) antenna temperatures for the *F-15* 22V channel.

instrument failed in August 2008, resulting from an electrical malfunction that rendered the spacecraft data recorder inoperable.

6) *F-15* SATELLITE

The *F-15* SSM/I 22V channel characteristics were found to be indicative of other channels, with two exceptions. The 22V channel appeared to have severe RADCAL beacon contamination (in a publicly undocumented Navy-conducted test) in 2009 (as of 15 April 2009), as shown in Fig. 14. RADCAL testing started in August 2006, but was not observable through this study's temperature analysis until the second major testing started in February 2009, as shown in Figs. 14b,c, where strong negative z scores or widely varying temperatures were observed. The second exception was the positive trend found in cold–warm calibration counts and corresponding temperatures, as depicted in Figs. 14a,c, respectively, started in late 2006 for this channel, but no similar trends were discernable with the other channels. The same issues found in *F-13* and *F-14* SSM/I channels between late 2003 through 2008 were also found for all *F-15* SSM/I channels, strongly supporting the argument that ground station processing may have caused this suspicious data and not individual instrument issues. The z scores between ± 10, shown in Fig. 14b, were found to be a reasonable threshold to use to identify the most suspicious data for user needs.

4. Conclusions

The application of z scores and threshold parameters (radiance, temporal, and geolocation-expected range checks) in the form of embedded quality flags has improved the scientific maturity of the SSM/I TDR/SDR period of record for climatological applications. The reprocessing of the SSM/I period of record to a self-describing standard format (netCDF) and file-level improvements have also helped to preserve the longest satellite passive microwave period of record. It was found that errors and suspicious data in the calibration count records account for most of the data quality issues in the SSM/I radiance period of record. This work is a key first step before a complete intercalibration and homogenization of the SSM/I period of record can be undertaken under NOAA's SDS program. The development of a SSM/I and SSMIS FCDR and associated TCDR datasets are projected to occur in the next few years.

Acknowledgments. We thank Gary Wick at NOAA ESRL for his guidance, and we thank the peer reviewers, whose comments were essential in improving this paper.

REFERENCES

Belchansky, G. I., D. C. Douglas, V. A. Eremeev, and N. G. Platonov, 2005: Variations in the Arctic's multiyear sea ice cover: A neural network analysis of SMMR-SSM/I data, 1979–2004. *Geophys. Res. Lett.,* **32,** L09605, doi:10.1029/2005GL022395.

Berg, W., and C. Kummerow, 2006: Common calibrated brightness temperature data file specification. Release 1.0. 9 pp. [Available online at http://mrain.atmos.colostate.edu/LEVEL1C/doc/SSMI_L1C_Specification.pdf.]

Colton, M., and G. Poe, 1999: Intersensor calibration of DMSP SSM/Is: F-8 to F-14; 1987-97. *IEEE Trans. Geosci. Remote Sens.,* **37,** 418–439.

Ferraro, R. R., F. Weng, N. C. Grody, and A. Basist, 1996: An eight-year (1987–1994) time series of rainfall, clouds, water vapor, snow cover, and sea ice derived from SSM/I measurements. *Bull. Amer. Meteor. Soc.,* **77,** 891–905.

——, E. A. Smith, W. Berg, and G. Huffman, 1998: A review of screening techniques for passive microwave precipitation retrieval algorithms. *J. Atmos. Sci.,* **55,** 1583–1600.

Huffman, G. J., and Coauthors, 1996: The Global Precipitation Climatology Project (GPCP) Combined Precipitation Data Set. *Bull. Amer. Meteor. Soc.,* **78,** 5–20.

Jackson, T. J., A. Y. Hsu, and P. E. O'Neill, 2002: Surface soil moisture retrieval and mapping using high-frequency microwave satellite observations in the Southern Great Plains. *J. Hydrometeor.,* **3,** 688–699.

Lawrence Livermore National Laboratory, cited 2009: CF metadata: NetCDF climate and forecast metadata convention. [Available online at http://cf-pcmdi.llnl.gov.]

National Research Council, 2004: *Climate Data Records from Environmental Satellites*. National Research Council of the National Academies, 150 pp.

Raytheon, 2000: Special Sensor Microwave/Imager user's interpretation guide. Developed for DMSP Program Office, USAF Space and Missile Systems Center, 96 pp.

Serreze, M. C., J. A. Maslank, R. H. Preller, and R. G. Barry, 1990: Sea ice concentrations in the Canada basin during 1988—Comparisons with other years and evidence of multiple forcing mechanisms. *J. Geophys. Res.,* **95,** 253–267.

UCAR Unidata, cited 2009: NetCDF. [Available online at http://www.unidata.ucar.edu/software/netcdf/.]

Vila, D., R. R. Ferraro, and H. Semunegus, 2010: Improved global rainfall retrieval using the Special Sensor Microwave Imager (SSM/I). *J. Appl. Meteor. Climatol.,* in press.

Weng, F., and N. C. Grody, 1998: Physical retrieval of land surface temperature using the Special Sensor Microwave Imager. *J. Geophys. Res.,* **103,** 8839–8848.

Zhang, H.-M., J. J. Bates, and R. W. Reynolds, 2006: Assessment of composite global sampling: Sea surface wind speed. *Geophys. Res. Lett.,* **33,** L17714, doi:10.1029/2006GL027086.